Vol. 75: 23–31, 2018
https://doi.org/10.3354/cr01506

CLIMATE RESEARCH
Clim Res

Published online March 21

Inter-annual variability of moisture transport over the northern Indian Ocean and South Asian summer monsoon

F. S. Syed[1,2,*], A. Hannachi[3]

[1]Directorate General of Climate Services, The General Authority of Meteorology and Environmental Protection (GAMEP), 21577 Jeddah, Kingdom of Saudi Arabia

[2]Institute of Meteorology and Geophysics (IMG), Pakistan Meteorological Department, 75270 Karachi, Pakistan

[3]Department of Meteorology, Stockholm University, 10691 Stockholm, Sweden

ABSTRACT: We studied the inter-annual variability of the vertically integrated zonal/meridional moisture transport in the lower troposphere over the northern Indian Ocean using observed data from 1971–2016 for the South Asian summer monsoon (SASM) season. The moisture transport variability was dominated by the zonal component associated with the Somali low level jet. For identification of the dominant modes of inter-annual variability, 3-dimensional empirical orthogonal function analysis was performed. The leading mode, associated with suppressed meridional moisture transport in both the Arabian Sea and Bay of Bengal and increased zonal moisture transport over the Bay of Bengal, was linked with the positive phase of the Indian Ocean dipole and El Niño conditions in the Pacific Ocean. The second leading mode was associated with the enhanced zonal moisture flow over the Arabian Sea extending up to the Bay of Bengal allied with the Somali low level jet, and enhanced northeastward moisture transport over the whole region. This enhanced moisture flow results in stronger monsoon circulation and increased rainfall over South Asia.

KEY WORDS: Inter-annual variability · Monsoon · Moisture transport · IOD · ENSO · South Asia

1. INTRODUCTION

Moisture transport (June–September; JJAS) over the Indian Ocean plays a fundamental role in determining South Asian summer monsoon (SASM) rainfall. Puranik et al. (2014) showed that during above-normal monsoon years, moisture transport is almost one order of magnitude more than that during below-normal rainfall years. Water vapor from south of equatorial Indian Ocean is the main source of the moisture for summer rainfall over continental regions of South Asia (Saha & Bavadekar 1973, Cadet & Reverdin 1981, Cadet & Greco 1987). It has been observed that 70% of the water vapor amount that reaches the west coast of India comes from the Southern Hemisphere through the Somali low level jet (SLLJ) and 30% comes from evaporation arising from the Arabian Sea, i.e. the inter-hemispheric moisture flux is larger than that from the Arabian Sea (Cadet & Reverdin 1981, Cadet & Greco 1987). Nevertheless, evaporation from the Arabian Sea is still an important moisture source for SASM rainfall (Ghosh et al. 1978, Murakami et al. 1984, Sadhuram & Ramesh Kumar 1988, Levine & Turner 2012).

Maximum transport occurs in the lower troposphere (between 1000 and 650 hPa) during the monsoon season, and maximum transport of moisture across the equator occurs in the months of June, July and August, between 42° and 60° E (Puranik et al. 2014). During the summer monsoon season, eastern and northeastern India receive moisture transported mainly by the northward branch of monsoon winds

*Corresponding author: faisal.met@gmail.com

from the Bay of Bengal. Although winds from the Arabian Sea may cross the eastern coast of India into the Bay of Bengal, the air over northeast India during the monsoon season generally originates over the Bay of Bengal (Konwar et al. 2012). Rainfall along the Western Ghats mountain range (west coast of India) results due to the uplifting of moisture brought by the SLLJ from cross-equatorial flow in the western Indian Ocean and Arabian Sea. Northern Pakistan and northwestern regions of India receive rainfall from the low pressure systems moving towards the west along the monsoon trough from the Bay of Bengal. These low pressure systems also pull moisture directly from the Arabian Sea (Latif et al. 2017).

A slight variation in inter-annual SASM rainfall can significantly impact agricultural production and water availability in the region (Turner & Annamalai 2012). A large part of the potential predictability of SASM is believed to be linked to forcing from the tropical oceans, especially the Pacific and Indian oceans, because of the fact that tropical oceans act as slowly varying boundary conditions of the atmosphere. Several studies (e.g. Kripalani et al. 1997, Li et al. 2008, Syed et al. 2010, 2012) have also suggested an extra-tropical influence on SASM variability. The El Niño-Southern Oscillation (ENSO) is one of the most important drivers of SASM variability because of its impacts around the globe through teleconnections (e.g. Trenberth et al. 1998, Alexander et al. 2002, Deser et al. 2004, Syed & Kucharski 2016). The teleconnection mechanism for the ENSO influence on SASM has been extensively studied (e.g. Webster & Yang 1992, Goswami 1998, Fasullo & Webster 2002) and relies on a modification of the Walker circulation with the shift of the deep convection and upper-level divergence from the western Pacific to the central Pacific region (e.g. Webster & Yang 1992, Ju & Slingo 1995, Kucharski et al. 2011). However, the ENSO–SASM relationship has weakened in the past decades (Kumar et al. 1999). The Indian Ocean dipole (IOD) also influences SASM rainfall variability (e.g. Cherchi & Navarra 2013). Some studies have shown that the IOD plays a role in the modification of ENSO teleconnection to SASM rainfall variability (Ashok et al. 2004, Ashok & Saji 2007). The IOD and the ENSO have complementarily affected SASM rainfall during the last 4 decades (Ashok et al. 2001). Generally, when the ENSO–SASM correlation is low, the IOD–SASM correlation is high, and vice versa. However, Syed & Kucharski (2016) showed that ENSO and IOD are not completely independent modes of variability on a seasonal inter-annual time scale.

Many studies have focused on the asymmetric trends in the seasonal mean JJAS SASM rainfall over different sub-regions of South Asia (Konwar et al. 2012, Kulkarni 2012, Roxy et al. 2015, Latif et al. 2017). These trends have been attributed to contrasting trends in meridional moisture transport (MMT) over the Arabian Sea and Bay of Bengal (Konwar et al. 2012, Latif et al. 2017). Konwar et al. (2012) used European Centre for Medium-Range Weather Forecasts (ECMWF) Re-Analysis Interim (ERA-Interim) reanalysis data from 1979–2010 and showed that the trend of spatially averaged vertically integrated moisture transport over the Bay of Bengal is decreasing at −0.26 kg m^{-1} s^{-1} during JJAS, while over the Arabian Sea, it is increasing at the pace of 0.57 kg m^{-1} s^{-1} over JJAS. Both the zonal and MMT components contribute to the increasing trend in moisture transport over the Arabian Sea and decreasing trend over the Bay of Bengal (Konwar et al. 2012, Latif et al. 2017). However, the inter-annual variability of zonal moisture transport (ZMT) and MMT over Arabian Sea and Bay of Bengal has not been given much attention. The objective of this study was to unravel the relationship between moisture transport and SASM rainfall variability on a seasonal inter-annual time scale and identify the large-scale teleconnections in the tropical oceans governing this variability.

2. DATA AND METHODS

For moisture transport (surface pressure, specific humidity and winds), the monthly mean re-analysis data of National Centers for Environmental Prediction NCEP/NCAR (Kalnay et al. 1996) with a horizontal resolution of 2.5° × 2.5° were used. Climatic Research Unit CRU TS3.22 monthly precipitation data set (Harris et al. 2014) for the period 1971–2014 with a 0.5° × 0.5° grid resolution were used. In addition, we also used the global (1° × 1°) HadISST sea surface temperature (SST) data set (Rayner et al. 2003) for the period 1971–2016.

In the present study, the vertically integrated ZMT and MMT over the northern Indian Ocean were computed following Saha & Bavadekar (1973):

$$\mathrm{ZMT} = \frac{1}{g}\int_{P_s}^{P_{top}} q.u\ dP \quad (1)$$

$$\mathrm{MMT} = \frac{1}{g}\int_{P_s}^{P_{top}} q.v\ dP \quad (2)$$

where P is pressure (hPa), u and v are the zonal and meridional wind components (m s^{-1}), q is specific humidity (kg kg^{-1}), g represents acceleration due to

gravity (m s^{-2}), and *P*s and *P*top are pressure at the bottom or surface and top of the vertical levels respectively. Using the prescribed formula (Eq. 1), computations were carried out from a 1000–500 hPa pressure level, over the region 30° S–40° N and 40–100° E. All analyses were performed on the vertically integrated moisture transport (VIMT) in this study.

Three-dimensional (3D) empirical orthogonal function (EOF) analysis (e.g. Hannachi 1997, Hannachi et al. 2007) and principal component (PC) correlations were done on detrended seasonal mean JJAS rainfall anomaly data from 1971–2016. Together, the fields ZMT and MMT form a 3D field (2 spatial dimensions and 2 variables). For example, if we have data matrices **A** ($\boldsymbol{N} \times \boldsymbol{M}$) for ZMT and **B** ($\boldsymbol{N} \times \boldsymbol{M}$) for MMT, where $\boldsymbol{M}$ (columns) are grid points and $\boldsymbol{N}$ (rows) are observations, then by concatenating the 2 matrices we get a new larger data matrix **C** ($\boldsymbol{N} \times 2\boldsymbol{M}$) = [**A B**]. Then, EOF analysis is done on the matrix **C**. The first EOF is a vector of size $2\boldsymbol{M}$. The first $\boldsymbol{M}$ elements represent the ZMT part of EOF-1 and the last $\boldsymbol{M}$ elements represent the MMT part of EOF-1 of the vertically integrated moisture transport. Note that the ZMT and MMT parts of EOF-1 are plotted separately but they have same explained variance and same PCs; EOF-2 is plotted similarly.

3. RESULTS AND DISCUSSION

3.1. Mean ZMT and MMT in the Indian Ocean

The climatology of seasonal mean JJAS vertically integrated (1000–500 hPa) ZMT and MMT (kg m^{-1} s^{-1}) for the period 1971–2016 are shown in Fig. 1a,b. The zonal component of the moisture is much stronger than the meridional component, with ZMT values exceeding 350 kg m^{-1} s^{-1} over the Arabian Sea. The ZMT decreases as the SLLJ hits the Western Ghats over the Indian peninsula. There are clearly 2 maxima in MMT, with maximum values >200 kg m^{-1} s^{-1} over both regions, i.e. in the Bay of Bengal and the cross-equatorial flow along the SLLJ to the Arabian Sea. The moisture flows sporadically from the northern tip of Madagascar to the Kenyan coast (3° S). It then penetrates inland over the lowlands of Ethiopia and Somalia and emerges out into the Arabian Sea near 9° N. Our findings are consistent with Fasullo & Webster (2002) climatology (1958–2000) and transports of vertically integrated moisture across key boundaries in the Indian Ocean.

Over the Bay of Bengal, the MMT can be observed starting from the equator and extending inland up to the foothills of the eastern Himalayas (25° N). Fig. 1c shows the complete picture of moisture transport vectors with their magnitudes; clearly moisture transport in the northern Indian Ocean is associated with SLLJ. The climatology (1971–2016) of the vertical structure of MMT, zonally averaged over the Indian Ocean (40–100° E) shows that maximum transport occurs in the lower troposphere, below the 500 hPa level. The northward MMT starts from 30° S and the transport of moisture abruptly stops at 30° N due to the barrier of the Himalayan mountains (Fig. 1d).

We first examined the relationship between the seasonal inter-annual moisture transport over the Bay of Bengal and the cross-equatorial moisture flow to the Arabian Sea. The time series of spatially averaged seasonal JJAS MMT for both cross-equatorial moisture transport into the Arabian Sea (0–22° N and 40–75° E) and Bay of Bengal (0–22° N and 80–100° E) from 1971–2016 are shown in Fig. 2. The MMT over the Arabian Sea shows an increasing trend, whereas a decreasing trend in MMT over the Bay of Bengal can be observed. Latif et al. (2017) showed a clear asymmetry with significant increased (decreased) MMT in the Arabian Sea (Bay of Bengal) respectively. However, trends in the MMT are not the focus of this study. Interestingly, there is no significant correlation between the 2 detrended time series (also in the case of ZMT, i.e. on the seasonal inter-annual time scale, Correlation of ZMT/MMT over the Arabian Sea and Bay of Bengal are not significantly correlated). The correlation between the Arabian Sea MMT detrended time series with SST indicates a La Niña-type pattern over Pacific Ocean, whereas the correlation of the detrended time series of MMT over Bay of Bengal and SST shows an El Niño-type pattern. Correlation of ZMT over the Arabian Sea with SST shows a negative IOD pattern over the Indian Ocean along with a La Niña-type pattern in the Pacific Ocean (data not shown), whereas ZMT over the Bay of Bengal does not show any clear pattern in the tropical SSTs (data not shown). In order to further investigate the coupled patterns of variability in ZMT and MMT over the northern Indian Ocean, we performed a 3D empirical orthogonal function (3D-EOF) analysis in the next section.

3.2. Spatio-temporal features of inter-annual moisture transport variability

3D-EOF analysis (e.g. Hannachi 1997, Hannachi et al. 2007) was performed on ZMT and MMT over the

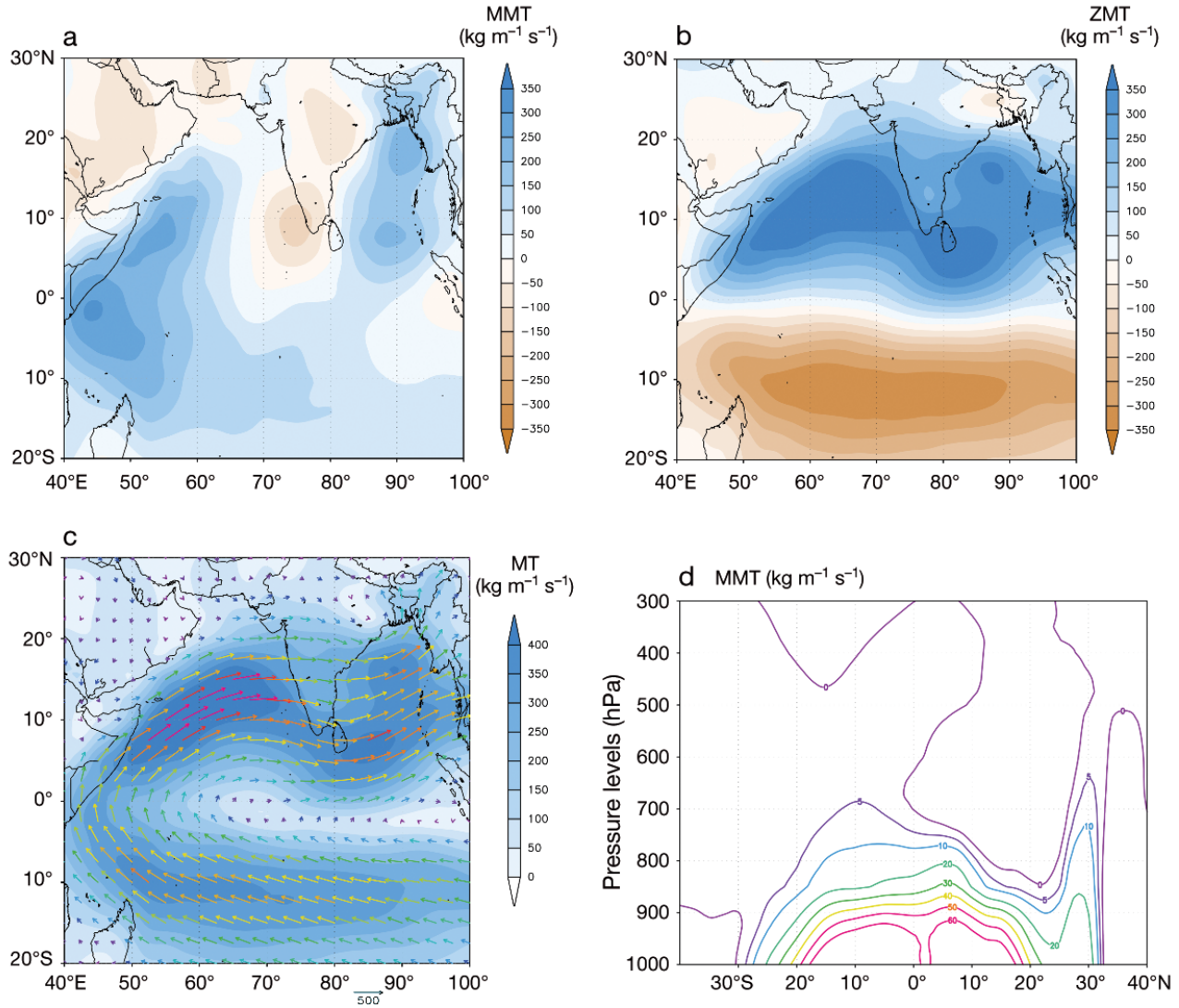

Fig. 1. Climatology (1971–2016) of June–September (JJAS) vertically integrated (a) meridional moisture transport (MMT), (b) zonal moisture transport (ZMT) and (c) moisture transport (MT); shading and vector colors (blue to red) represent the magnitude of moisture transport. (d) Zonally averaged (40–100° E) MMT vertical structure

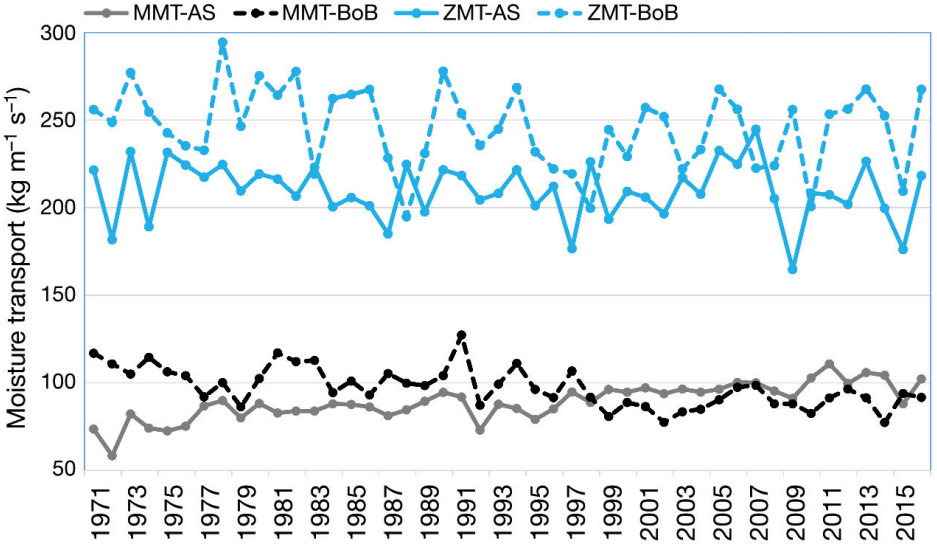

Fig. 2. Spatially averaged June–September (JJAS) vertically integrated (1000–500 hPa) meridional moisture transport (MMT) and zonal moisture transport (ZMT) for both the Arabian Sea (AS; 0–22° N and 40–75° E) and Bay of Bengal (BoB; 0–22° N and 80–100° E) from 1971–2016

northern Indian Ocean domain (0–35° N, 40–100° E). The eigenvalue spectrum of covariance matrix is shown in Fig. 3, with uncertainty estimates based on the North et al. (1982) rule of thumb. The leading 2 eigenvalues are clearly well separated from the rest of the spectrum, thus can be analyzed separately. Fig. 4a,b shows the leading pattern (EOF-1) of seasonal (JJAS) ZMT and MMT combined over the northern Indian Ocean, with 25.1% of explained variance. Since the sign of EOFs is irrelevant, we discuss below one phase ('positive phase') of the pattern. The first EOF is dominated by the zonal moisture flow; a north–south dipole pattern can be seen over the eastern part of the domain, with positive values of ZMT (northward flux) over the northern Bay of Bengal associated with negative values of MMT (southward flux) over western Arabian sea and Bay of Bengal, i.e. decreased northward moisture flux into the South Asian mainland. Conversely, a negative moisture flux over the Bay of Bengal is associated with a positive moisture flux over the western Arabian Sea and Bay of Bengal. The EOF-1 vectors and moisture convergence (Fig. 4c) clearly show a high circulation over southern India and the Bay of Bengal. If this circulation is compared with the mean moisture transport (Fig. 1c), it can be seen that the moisture transport from the Bay of Bengal into the mainland can be reduced or enhanced. It is interesting to note the north–south dipole in moisture convergence over the Bay of Bengal. We shall see in the next section that this center of action for variability in moisture transport into the south Asian mainland is associated with El Niño and a positive IOD phenomenon in the Pacific and Indian Oceans respectively. The positive phase of the

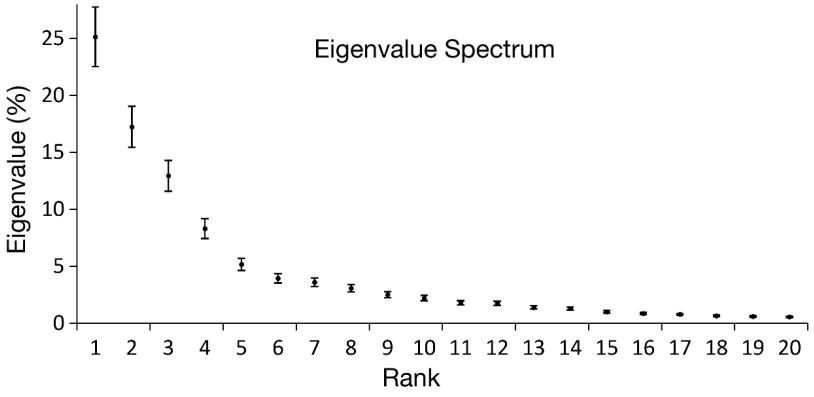

Fig. 3. Spectrum of the covariance matrix of summer (June–September; JJAS) mean vertically integrated moisture transport. Vertical bars show uncertainty estimates based on the North et al. (1982) rule of thumb. Only the leading 20 eigenvalues are shown

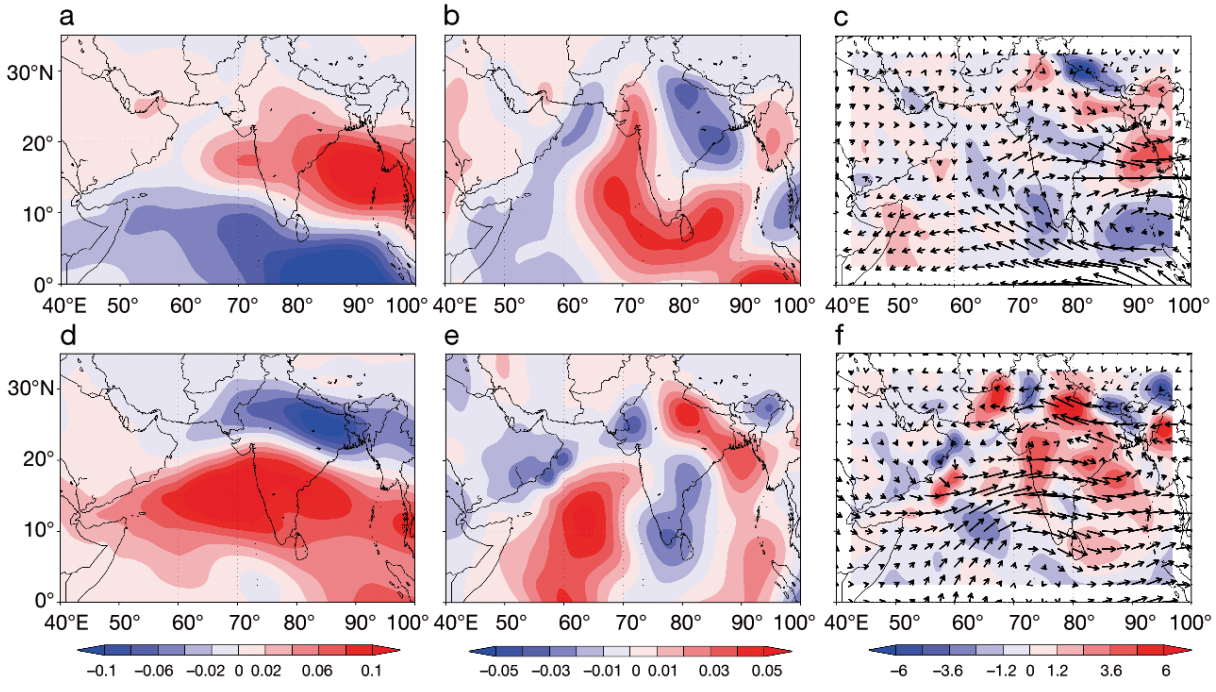

Fig. 4. (a) Zonal and (b) meridional parts of the first empirical orthogonal function (EOF-1) of summer (June–September; JJAS), vertically integrated (1000–500 hPa) zonal moisture transport (ZMT) and meridional moisture transport (MMT), explained variance 25.1%. (c) The vector form of EOF-1 (arrows) and convergence of EOF-1 (shading). (d–f) are the same as (a–c), but for EOF-2, explained variance 17.2%

second EOF, with 17.2% explained variance, is related to enhanced monsoon circulation (Fig. 4f). Unlike the first EOF, the centers of action in EOF-2 are shifted over mainland. In the positive phase (shown in Fig. 4) of EOF-2, the ZMT is stronger over the Arabian Sea and there is strong zonal moisture flow into the Indian peninsula (Fig. 4d). The corresponding pattern of EOF-2 in the case of MMT also shows enhanced flow of moisture in the Arabian Sea as well as in the Bay of Bengal. Enhanced northwards moisture flow can also be seen along the foothills of the Himalayas. In the next section we discuss the global teleconnections related to these EOF patterns and their influence on SASM variability.

3.3. Teleconnections and moisture transport inter-annual variability

The NINO3.4 index records average SST anomalies in the Pacific (5° S–5° N and 170–120° W) and is used to classify SST variability in the Pacific related to ENSO. Thus, El Niño- (La-Niña)-type conditions in the Pacific correspond to positive (negative) values of the NINO3.4 index. We characterized the variability of SST anomalies over the equatorial Indian Ocean by using the IOD index. We followed Saji et al. (1999) in order to define the IOD index as the difference in SST anomalies between the tropical western Indian Ocean (10° S–10° N, 50–70° E) and the tropical southeastern Indian Ocean (10–0° S, 90–110° E). A positive IOD index describes cooler than normal water in the tropical eastern Indian Ocean and warmer than normal water in the tropical western Indian Ocean, and vice versa. The correlation between the IOD index and NINO3.4 index is 0.51, and Syed & Kucharski (2016) showed that neither phenomena are completely independent on a seasonal inter-annual time scale.

The PCs of the first 2 leading EOF modes of vertically integrated moisture transport were correlated with global SSTs from 30° S–30° N (Fig. 5). The first mode (Fig. 5a) pattern shows an El Niño-type structure in the tropical Pacific Ocean and also a positive IOD pattern in the Indian Ocean. The correlation of PC1 with NINO3.4 index is 0.5 and with IOD index is 0.7; both values are significant at the 1% level. Note here that sign is irrelevant, but the obtained patterns (Fig. 5) are to be discussed in association with the positive phase of EOF-1 and EOF-2 shown in Fig. 4. This indicates that the positive phase of ENSO and IOD are generally related to suppressed monsoon circulation (Fig. 4c) and vice versa. However, this is not true for all years; Gadgil et al. (2004) showed that if either of ENSO or IOD conditions are unfavorable, then the monsoon fails. The correlation of PC2 with global SSTs shows negative values in the northern Indian Ocean and eastern Pacific Ocean; La Niña-type structure is clearly visible in the Pacific Ocean (Fig. 5b). The correlation between PC2 and the IOD

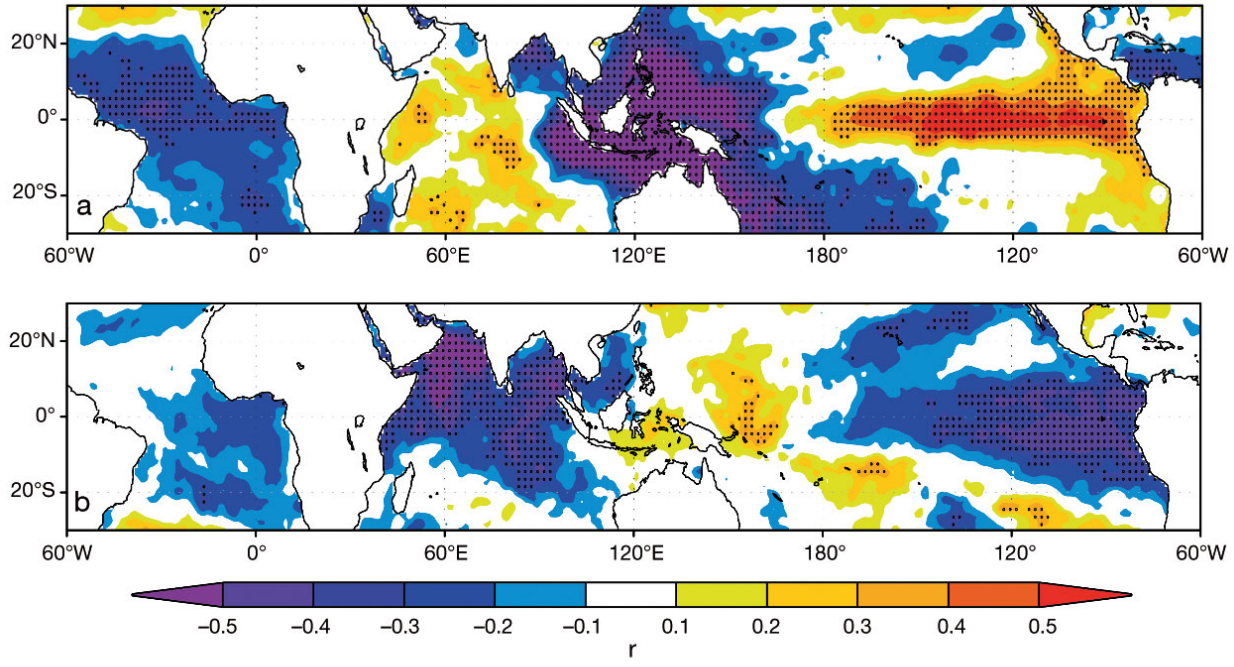

Fig. 5. Correlation (1971–2016) of summer (June–September; JJAS) sea surface temperatures (SSTs) with (a) PC1 and (b) PC2. Stippling shows statistically significant correlation values at 95% confidence level

index is not statistically significant, and the correlation with the NINO3.4 index is 0.31. This suggests that La Niña (El Niño) is the only major phenomenon in the tropical oceans associated with enhanced (reduced) monsoon circulation. La Niña seems to strengthen the SLLJ, especially over the Arabian Sea, and enhances the northwards moisture transport over the Arabian Sea and Bay of Bengal. Syed & Kucharski (2016) performed a maximum covariance analysis between global tropical SSTs and SASM rainfall and showed that ENSO is the leading mode in the tropics associated with inter-annual variability in SASM rainfall, whereas the eastern pole of the IOD contributes to the second global mode in the tropics and is the leading mode in the Indian Ocean. They also showed that on a seasonal JJAS inter-annual time scale, IOD is not a completely separate independent mode of variability in the Indian Ocean, but is also associated with ENSO.

To further examine the relationship of these 2 leading EOF modes of variability with SASM rainfall, we correlated the PCs with mean JJAS SASM rainfall. The mean climatology of SASM rainfall is shown in Fig. 6a. The monsoon penetrates into northern Pakistan along the foothills of the Himalayas from India, but the mean monsoon rainfall remains below 200 mm over northern India and Pakistan. Mean seasonal precipitation is >500 mm over the Western Ghats and the contiguous land areas of the Bay of Bengal. Central India also receives a good amount of rainfall; mean rainfall is between 200–300 mm. Fig. 6b shows the correlation between PC1 and SASM rainfall. The

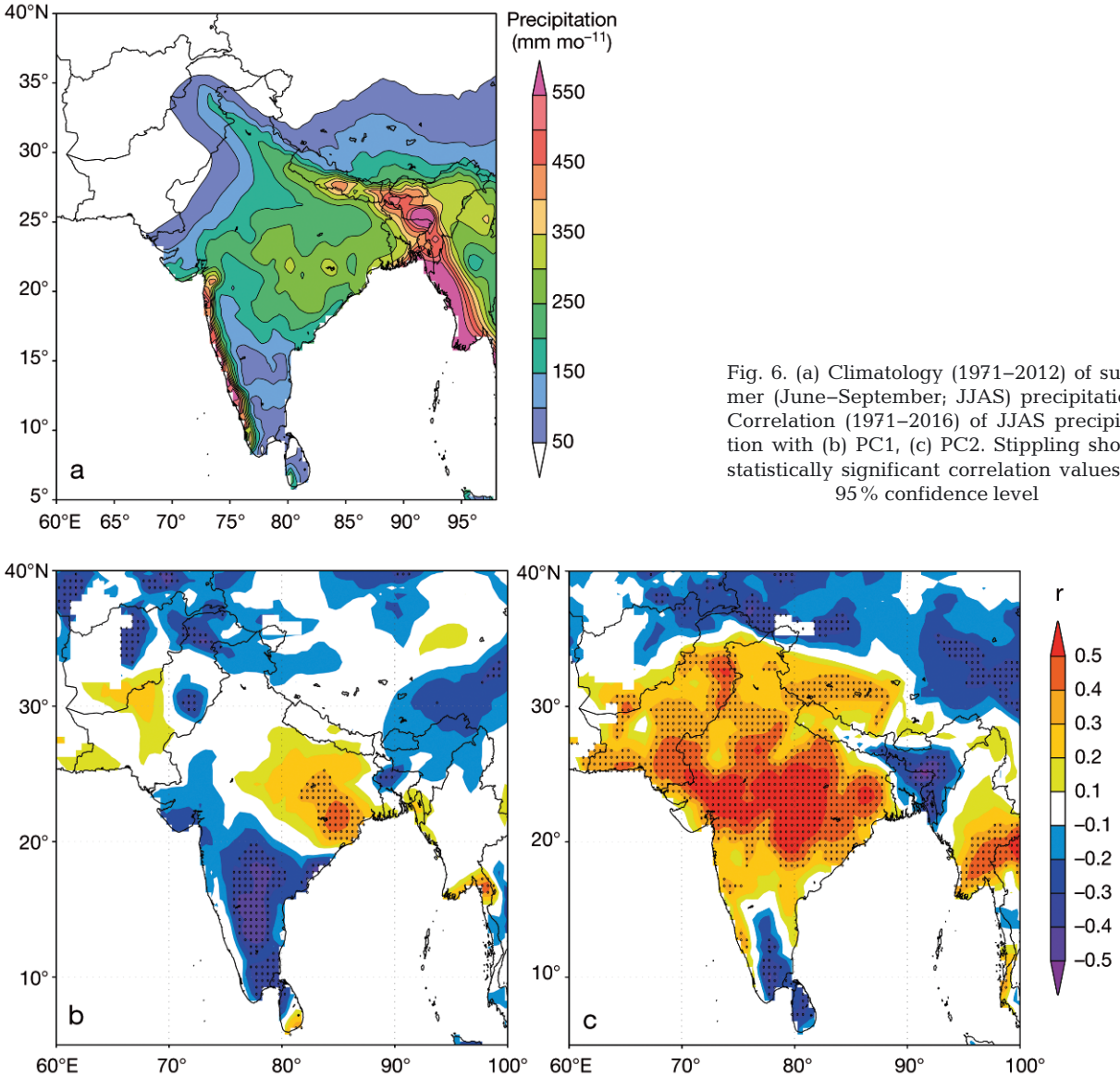

Fig. 6. (a) Climatology (1971–2012) of summer (June–September; JJAS) precipitation. Correlation (1971–2016) of JJAS precipitation with (b) PC1, (c) PC2. Stippling shows statistically significant correlation values at 95% confidence level

leading mode ('positive phase') showing decreased MMT over both the Arabian Sea and Bay of Bengal (Fig. 4b), which is associated with a combination of a positive (negative) ENSO and a positive (negative) IOD signal in SSTs, is related to generally decreased (increased) rainfall over South Asia. The decrease in rainfall over southern India is particularly visible (Fig. 6b). The second mode of EOF variability showing increased (decreased) MMT over the Bay of Bengal, which is related to a negative (positive) ENSO pattern in the Pacific Ocean, is associated with increased (decreased) rainfall over South Asia. It is worth mentioning here that the spatial correlation of atmospheric fields, e.g. SST or precipitation, enhances the statistical significance observed, for example with regards to the spatial correlations for Figs. 5 & 6 (Delsole & Yang 2011, Wilks 2016). This does not, however, affect the general message of the above discussion. We also performed EOF analysis of ERA-interim data and found similar leading modes of variability, which shows the robustness of our results.

4. SUMMARY AND CONCLUSIONS

We investigated the climatological features and inter-annual variability of zonal and meridional moisture fields in the northern Indian Ocean and the relationship between ZMT and MMT associated with SASM rainfall over South Asia and tropical SST variability in the Indian and Pacific Oceans, based on the NCEP/NCAR reanalysis and observed rainfall from 1971–2015. Two maxima exist in the climatology of MMT, with a maximum value above 200 kg m^{-1} s^{-1} over the Bay of Bengal and the cross-equatorial flow along the SLLJ into the Arabian Sea. The maximum ZMT occurs over the Arabian Sea, with values exceeding 300 kg m^{-1} s^{-1}. The ZMT and MMT over the Arabian Sea and Bay of Bengal are not correlated on a seasonal mean inter-annual time scale (when detrended). The climatology (1971–2015) of the vertical structure of MMT shows maximum transport occurring in the lower troposphere, below the 500 hPa level. The northward MMT starts from south of the equator and goes north up to the Himalayan mountains.

Three-dimensional EOF analysis showed that the leading mode is associated with suppressed or weak MMT in both the Arabian Sea and Bay of Bengal. However, increased ZMT is observed over the Bay of Bengal, which results in the weakened monsoon circulation and decreased moisture convergence. The positive phase of the leading mode of 3D-EOF is associated with the positive phase of the IOD in the Indian Ocean and El Niño conditions in the Pacific Ocean, which results in the suppressed SASM rainfall. The positive phase of the second mode of 3D-EOF is associated with La Niña conditions in the Pacific Ocean, which results in the enhanced zonal moisture flow over the Arabian Sea extending up to the Bay of Bengal allied with the SLLJ, and enhanced northward moisture transport over the whole region. This enhanced moisture flow marks stronger monsoon circulation and increased rainfall over South Asia.

This study provides the basic information about the moisture transport climatology and its modes of variability on an inter-annual time scale, and how this variability is associated with the SASM rainfall. The method adopted (3D-EOF analysis) in this study would also be useful for other climate variability studies dealing with the variability of more than one field together.

Acknowledgements. F.S.S. thanks the International Meteorological Institute (IMI) for sponsoring the visit to the Department of Meteorology, Stockholm University, Sweden, for this study.

LITERATURE CITED

Alexander MA, Blade I, Newman M, Lanzante JR, Lau NC, Scott JD (2002) The atmospheric bridge: the influence of ENSO teleconnections on air-sea interaction over the global oceans. J Clim 15:2205–2231

Ashok K, Saji NH (2007) On impacts of ENSO and Indian Ocean dipole events on the sub-regional Indian summer monsoon rainfall. Nat Hazards 42:273–285

Ashok K, Guan Z, Yamagata T (2001) Impact of the Indian Ocean dipole on the relationship between the Indian monsoon rainfall and ENSO. Geophys Res Lett 28: 4499–4502

Ashok K, Guan Z, Saji NH, Yamagata T (2004) Individual and combined influences of the ENSO and Indian Ocean dipole on the Indian summer monsoon. J Clim 17: 3141–3155

Cadet D, Greco S (1987) Water vapor transport over the Indian Ocean during the 1979 summer monsoon. I. Water vapor fluxes. Mon Weather Rev 115:653–663

Cadet D, Reverdin G (1981) Water vapour transport over the Indian Ocean during summer 1975. Tellus 33:476–487

Cherchi A, Navarra A (2013) Influence of ENSO and of the Indian Ocean dipole on the Indian summer monsoon variability. Clim Dyn 41:81–103

Delsole T, Yang X (2011) Field significance of regression patterns. J Clim 24:5094–5107

Deser C, Phillips AS, Hurrell JW (2004) Pacific interdecadal climate variability: linkages between the tropics and the North Pacific during boreal winter since 1900. J Clim 17: 3109–3124

Fasullo J, Webster PJ (2002) Hydrological signatures relating the Asian summer monsoon and ENSO. J Clim 15: 3082–3095

Gadgil S, Vinayachandran PN, Francis PA, Gadgil G (2004) Extremes of the Indian summer monsoon rainfall, ENSO and equatorial Indian Ocean oscillation. Geophys Res Lett 31:L12213

Ghosh SK, Pant CM, Dewan BN (1978) Influence of the Arabian Sea on Indian summer monsoon. Tellus 30:117–125

Goswami BN (1998) Interannual variations of Indian summer monsoon in a GCM: external conditions versus internal feedbacks. J Clim 11:501–522

Hannachi A (1997) Low frequency variability in GCM: 3D flow regimes and their dynamics. J Clim 10:1357–1379

Hannachi A, Jolliffe IT, Stephenson DB (2007) Empirical orthogonal functions and related techniques in atmospheric science: a review. Int J Climatol 27:1119–1152

Harris I, Jones PD, Osborn TJ, Lister DH (2014) Updated high-resolution grids of monthly climatic observations — the CRU TS3.10 dataset. Int J Climatol 34:623–642

Ju J, Slingo JM (1995) The Asian summer monsoon and ENSO. QJR Meteorol Soc 121:1133–1168

Kalnay E, Kanamitsu M, Kistler R, Collins W and others (1996) The NCEP/NCAR 40-year reanalysis project. Bull Am Meteorol Soc 77:437–471

Konwar M, Parekh A, Goswami BN (2012) Dynamics of east-west asymmetry of Indian summer monsoon rainfall trends in recent decades. Geophys Res Lett 39: L10708

Kripalani RH, Kulkarni A, Singh SV (1997) Association of the Indian summer monsoon with the Northern Hemisphere mid-latitude circulation. Int J Climatol 17:1055–1067

Kucharski F, Kang IS, Farneti R, Feudale L (2011) Tropical Pacific response to 20th century Atlantic warming. Geophys Res Lett 38:L03702

Kulkarni A (2012) Weakening of Indian summer monsoon rainfall in warming environment. Theor Appl Climatol 109:447–459

Kumar KK, Rajagopalan B, Cane MA (1999) On the weakening relationship between the Indian monsoon and ENSO. Science 284:2156–2159

Latif M, Syed FS, Hannachi A (2017) Rainfall trends in the South Asian summer monsoon and its related large-scale dynamics with focus over Pakistan. Clim Dyn 48: 3565–3581

Levine RC, Turner AG (2012) Dependence of Indian monsoon rainfall on moisture fluxes across the Arabian Sea and the impact of coupled model sea surface temperature biases. Clim Dyn 38:2167–2190

Li S, Perlwitz J, Quan X, Hoerling MP (2008) Modelling the influence of North Atlantic multidecadal warmth on the Indian summer rainfall. Geophys Res Lett 35:L05804

Murakami T, Nakazawa T, He J (1984) On the 40–50 day oscillations during the 1979 northern hemisphere summer. II. Heat and moisture budget. J Meteorol Soc Jpn 62:469–484

North GR, Bell TL, Cahalan RF, Moeng FJ (1982) Sampling errors in the estimation of empirical orthogonal functions. Mon Weather Rev 110:699–706

Puranik SS, Ray KC, Sen PN, Kumar PP (2014) Impact of cross-equatorial meridional transport on the performance of the southwest monsoon over India. Current Sci 107:1006–1013

Rayner NA, Parker DE, Horton EB, Folland CK and others (2003) Global analyses of sea surface temperature, sea ice, and night marine air temperature since the late nineteenth century. J Geophys Res 108:D144407

Roxy MK, Ritika K, Terray P, Murtugudde R, Ashok K, Goswami BN (2015) Drying of Indian subcontinent by rapid Indian Ocean warming and a weakening land-sea thermal gradient. Nat Commun 6:7423

Sadhuram Y, Ramesh Kumar MR (1988) Does evaporation over the Arabian Sea play a crucial role in moisture transport across the west coast of India during an active monsoon period? Mon Weather Rev 116:307–312

Saha KR, Bavadekar SN (1973) Water vapour budget and precipitation over the Arabian Sea during the northern summer. QJR Meteorol Soc 99:273–278

Saji NH, Goswami BN, Vinayachandran PN, Yamagata T (1999) A dipole mode in the tropical Indian Ocean. Nature 401:360–363

Syed FS, Kucharski F (2016) Statistically related coupled modes of South Asian summer monsoon interannual variability in the tropics. Atmos Sci Lett 17:183–189

Syed FS, Yoo JH, Körnich H, Kucharski F (2010) Are intraseasonal summer rainfall events micro monsoon-onsets over the western edge of the South-Asian monsoon? Atmos Res 98:341–346

Syed FS, Yoo JH, Körnich H, Kucharski F (2012) Extratropical influences on the inter-annual variability of South-Asian monsoon. Clim Dyn 38:1661–1674

Trenberth KE, Branstator GW, Karoly D, Kumar A, Lau NC, Ropelewski C (1998) Progress during TOGA in understanding and modeling global teleconnections associated with tropical sea surface temperatures. J Geophys Res 14:291–324

Turner AG, Annamalai H (2012) Climate change and the South Asian summer monsoon. Nat Clim Chang 2: 587–595

Webster PJ, Yang S (1992) Monsoon and ENSO: selectively interactive systems. QJR Meteorol Soc 118:877–926

Wilks DS (2016) The stippling shows statistically significant gridpoints: how research results are routinely overstated and over-interpreted, and what to do about it. Bull Am Meteorol Soc 97:2263–2273

Editorial responsibility: Oliver Frauenfeld, College Station, Texas, USA

Submitted: July 17, 2017 ; Accepted: December 17, 2017
Proofs received from author(s): March 11, 2018